ACS chemical biology

Articles

Cite This: ACS Chem. Biol. 2019, 14, 1260−1270

pubs.acs.org/acschemicalbiology

Omics Technologies to Understand Activation of a Biosynthetic Gene Cluster in *Micromonospora* sp. WMMB235: Deciphering Keyicin Biosynthesis

Deepa Acharya,[†] Ian Miller,[†] Yusi Cui,[†] Doug R. Braun,[†] Mark E. Berres,[‡] Matthew J. Styles,[§] Lingjun Li,[†] Jason Kwan,[†] Scott R. Rajski,[†] Helen E. Blackwell,[§] and Tim S. Bugni*[,†]

[†]Pharmaceutical Sciences Division, University of Wisconsin—Madison, Madison, Wisconsin 53705, United States

[‡]Bioinformatics Resource Center, University of Wisconsin—Madison, Madison, Wisconsin 53706, United States

[§]Department of Chemistry, University of Wisconsin—Madison, Madison, Wisconsin 53706, United States

Supporting Information

ABSTRACT: DNA sequencing of a large collection of bacterial genomes reveals a wealth of orphan biosynthetic gene clusters (BGCs) with no identifiable products. BGC silencing, for those orphan clusters that are truly silent, rather than those whose products have simply evaded detection and cluster correlation, is postulated to result from transcriptional inactivation of these clusters under standard laboratory conditions. Here, we employ a multi-omics approach to demonstrate how interspecies interactions modulate the keyicin producing *kyc* cluster at the transcriptome level in cocultures of *kyc*-bearing *Micromonospora* sp. and a *Rhodococcus* sp. We further correlate coculture dependent changes in keyicin production to changes in transcriptomic and proteomic profiles and show that these changes are attributable to small molecule signaling consistent with a quorum sensing pathway. In piecing together the various elements underlying keyicin production in coculture, this study highlights how omics technologies can expedite future efforts to understand and exploit silent BGCs.

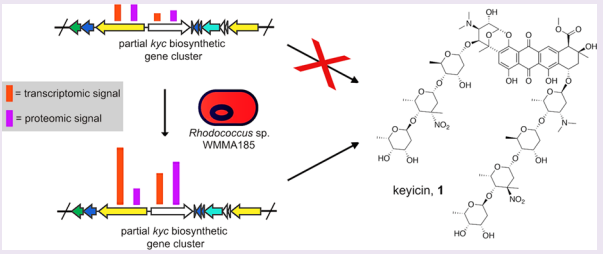

INTRODUCTION

One of the seminal findings in the arena of infectious disease over the last 20 years has been the realization that quorum sensing (QS) among microbial organisms plays a critical role in dictating how microbes govern themselves.[1−3] Microbial QS entails the generation of extracellular chemical signals, which accumulate in the local environment; once they reach a threshold concentration (and thus a "quorum" of cells has accumulated), the transcription of group-specific genes is activated. Ultimately, these QS-driven changes in transcription constitute the expression of group-beneficial behaviors, including but not limited to virulence and biofilm formation.[4] Accordingly, it comes as no surprise that numerous campaigns to devise new "antivirulence" agents have targeted bacterial QS systems.[5−7] Generally speaking and informed by the pressing global need to identify new antimicrobial agents, most QS systems studied thus far have involved intraspecies interactions. Indeed, this makes perfect sense as intraspecies interactions needed to gain a "quorum" would be expected of "self-governing" mechanisms needed for a group of cells to achieve common goals.

That said, it is in this *intraspecies* realm that QS has most recently captured the imaginations of drug discovery scientists by influencing microbial secondary metabolic pathways. In short, it is now clear that QS mechanisms offer one means of activating (or "de-repressing") otherwise silent biosynthetic gene clusters (BGCs) leading to the production of new natural products. For instance, elegant work by Hertweck and co-workers revealed the critical role that LuxR-based QS plays in silencing the biosynthesis of thailandamide A lactone in wild-type *Burkholderia thailandensis*.[8] Subsequent work by Seyedsayamdost and co-workers recently revealed that the QS-controlled transcriptional regulator ScmR serves as a global gatekeeper of secondary metabolism in *Burkholderia thailandensis* E264[9] and repressor of numerous BGCs, whereas Greenberg and co-workers have shown that QS in *B. thailandensis* impacts biosynthetic gene clusters that code for the synthesis of malleobactin, malleilactone, quinolones, rhamnolipids, and others.[10] Importantly, all of these QS systems are of the LuxI/LuxR class that is typical of Gram-negative bacteria.[11] These systems consist of a LuxI-type synthase that produces a diffusible *N*-acyl L-homoserine lactone (AHL) signal, and a LuxR-type receptor that binds the AHL and activates transcription of QS-controlled genes. AHLs constitute the extracellular chemical signals by which bacteria communicate en route to self-governance.[12−14] By extension, the relevance of *interspecies* associations to BGC activation processes holds tremendous promise and now

Received: March 20, 2019
Accepted: May 23, 2019
Published: May 23, 2019

DOI: 10.1021/acschembio.9b00223
ACS Chem. Biol. 2019, 14, 1260−1270

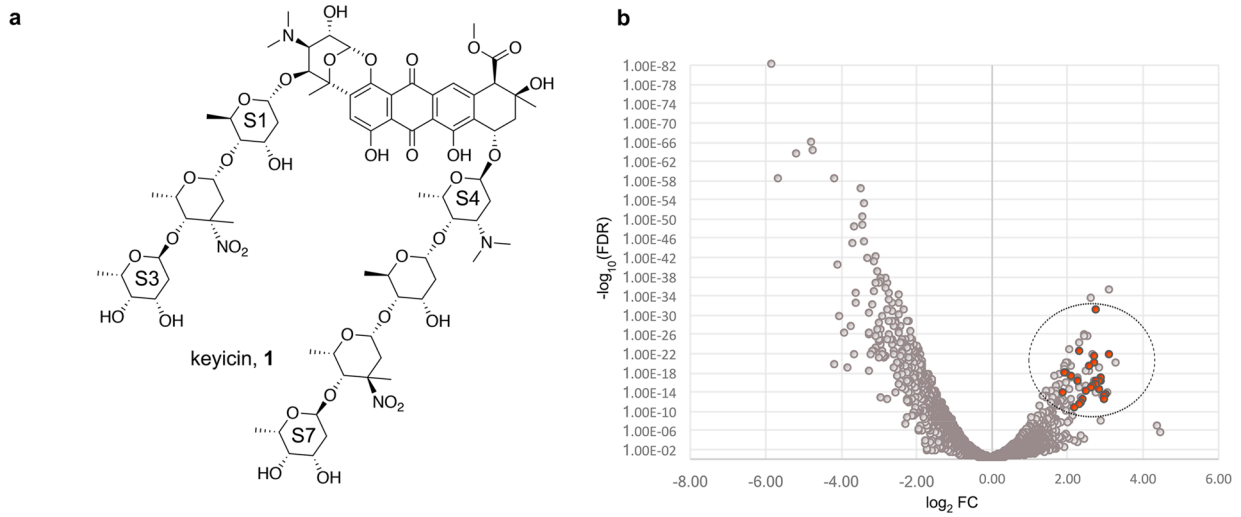

Figure 1. Structure of coculture-dependent polyketide keyicin **1** (a) and differential gene expression from WMMB235 genome in coculture with *Rhodococcus* sp. WMMA185 (b). Genes from the *kyc* gene cluster are indicated as red spheres within the circled (dashed lines) region.

constitutes an area of active investigation within our laboratory.

It is now clear that QS mechanisms offer one viable means by which to modulate the biosynthetic machineries housed within specific microbes. Specifically, the activation of otherwise silent or "orphan" BGCs is a particularly exciting application of QS pathways since it is now well established that microbial genetic diversity and possibilities far exceed previous expectations with respect to secondary metabolism and the natural product-based drug leads to which they give rise. For instance, a survey of only 1154 genomes revealed >10000 distinct biosynthetic gene clusters (BGCs), a number that is 10-fold greater than the *TOTAL number* of experimentally characterized BGC's currently in the MIBiG repository.[15−17] Alarmingly, no small molecule-to-BGC correlation can be made for the overwhelming majority of these clusters.[18−23]

Activation of silent BGCs (identified by genomics) has been achieved by (i) changing growth conditions, (ii) chemical elicitors, (iii) targeted genetic modifications, (iv) alterations to transcriptional machineries, and (v) heterologous expression methods;[22] although comprehensive correlations of natural product biosynthesis to changes in transcriptomics or proteomics have rarely been achieved. Genomic information alone, though useful from BGC mining initiatives, is insufficient to unveil and make available new secondary metabolites; transcriptomic, proteomic, and metabolomic data play indispensable roles in producing new structures from otherwise silent BGCs.

Coculturing different microbes has also been shown to activate silent BGCs,[24−28] and resulting metabolites are likely attributable to interspecies QS mechanisms that alter one or more of the factors noted above. Consistent with this notion, we recently reported that coculturing of *Micromonospora* sp. WMMB235 and a *Rhodococcus* sp. WMMA185 enabled the production of a new glycosylated anthracycline constructed by a large type II PKS, keyicin. Neither bacterium, in isolation, produced keyicin.[29] Despite the excitement and significance of this finding, little is known about how these organisms synergize to generate keyicin.

Early studies into keyicin production revealed WMMB235 as the producer of keyicin (**1**, Figure 1a) in coculture [see Figure S10, Supporting Information for statistical analysis (triplicates) via PCA].[29] This conclusion was supported primarily by two key findings. The first one was that only WMMB235 harbored a BGC (termed previously and herein *kyc*) able to code for all the machinery anticipated to be necessary for keyicin assembly; this was first illuminated upon PRISM[30] and AntiSmash[31−33] processing of the WMMB235 genome. Both analyses identified *kyc* as a large anthracycline type biosynthetic gene cluster housing several glycosyltransferases (GTs) envisioned as essential to keyicin assembly (Supporting Information). Second, fermentations in which the two microbial species were separated with a 0.2 μm cell impermeable membrane led, over time, to inhibited *Rhodococcus* sp. WMMA185 growth and increased keyicin production; this assay highlighted the antibacterial properties of keyicin as well as the absence of any required interspecies cell−cell contacts.[29]

We focus here on understanding how *Micromonospora* sp. WMMB235 and *Rhodococcus* sp. WMMA185 collaborate to produce keyicin via the application of genomics, transcriptomics, and proteomics technologies. We pay special attention to identifying biosynthetic bottleneck processes as well as keyicin analogs and how these findings might translate to other silent BGC systems. We also test the hypothesis that a LuxR-type receptor homologue, embedded within the keyicin BGC (*kyc*) dictates keyicin production in a fashion consistent with QS.

RESULTS AND DISCUSSION

Keyicin Production Is Small-Molecule-Triggered. To unequivocally determine the mode of interaction between WMMB235 and WMMA185, we expanded on the results of previously reported two chamber fermentation assays.[29] We found that keyicin production, as detected by colorimetric analyses (λ_{max} = 470 nm), from WMMB235 could be triggered simply by subjecting WMMB235 to supernatant from monocultured *Rhodococcus* sp. WMMA185. When inoculated into cell free media from a WMMA185 culture grown for 4 days, WMMB235 clearly generated **1** as reflected by production of keyicin's unique chromophore; the efficiency of keyicin production using WMMA185-derived supernatant was virtually identical to that seen in live coculture experiments, suggesting that nutrient depletion (by live WMMA185)

DOI: 10.1021/acschembio.9b00223
ACS Chem. Biol. 2019, 14, 1260−1270

exerts little to no influence upon the *kyc* machinery of WMMB235 (Figures S6 and S7, Supporting Information). This result clearly put to rest any possibility that WMMB235 and WMMA185 are involved in a dynamic communication system that requires both participants to be alive or active. Moreover, this experiment showed that WMMA185 produces a small molecule inducer of keyicin biosynthesis even in the absence of WMMB235, suggestive that QS may play an important, though not exclusive, role in triggering *kyc* BGC activation. Activation of keyicin biosynthesis by WMMB235 using only supernatants from monocultured WMMA185 also strongly affirms that keyicin biosynthesis is in response to a small molecule signal from WMMA185 and not a nutrient depletion or competition phenomenon.

Transcriptomic Activation of the *kyc* Cluster and Keyicin Production in Coculture. Early sequencing efforts made clear that keyicin assembly in coculture could be ascribed only to WMMB235.[29,34] To evaluate how *kyc* biosynthetic genes are impacted by the presence of WMMA185, we collected cells from days 2 and 5 of the cultures of WMMB235, WMMA185, and their coculture; LC/MS and colorimetric analyses (λ_{max} = 470 nm) revealed that keyicin was not produced in substantial quantities until day 4 of fermentation. Illumina sequencing of each mRNA collection enabled alignments of the resulting RNASeq data for the two genomes in order to parse transcript reads for WMMB235 (producer). The aggregate value of reads per kb/million reads aligning to annotated ORFs (RPKMO) of the gene clusters was calculated from the number of reads for each gene in the cluster that could be mapped to the genome.[35] This value was normalized to cluster length to ensure accurate representation of the smaller gene clusters in the genome relative to the large *kyc* cluster. Overall, the *kyc* cluster had RPKMO values of 1303.0 and 267 in monoculture on days 2 and 5, respectively. In coculture, the same RPKMO values were 1849.1 at day 2 and 2267.7 at day 5, consistent with significantly increased transcription of the *kyc* cluster in the presence of WMMA185 and the commensurate reduction of the same transcripts over time in monocultured WMMB235.

Further differential gene expression analyses (DGE) were conducted on day 5 data using EdgeR software[36] allowed us to quantitate the magnitude of differential expression of each WMMB235 gene in coculture relative to monoculture as a fold-change of read counts, along with the significance of this difference as adjusted *p*-value or false discovery rate (FDR). The volcano plot representative of this analysis (Figure 1b) revealed that, of all upregulated *orfs* within the complete WMMB235 genome, putative *kyc* cluster genes were among the most upregulated and had the lowest rates of false discovery. In fact, the vast majority of *orfs* within the *kyc* cluster showed at least a 2-fold (to the $\log_2$) increase in gene expression. These transcriptomic analyses suggested that the presence of WMMA185 induces the transcriptional activation of the *kyc* cluster. We posit that, in the absence of WMMA185, WMMB235 channels resources to other metabolic machineries unrelated to the assembly of **1**. These findings are critical to expanding our understanding of the "omics" behind keyicin production as well as the potential role that QS plays in *kyc* cluster activation in *Micromonospora* sp. WMMB235.

A Role for Quorum Sensing through LuxR in *kyc* Cluster Activation? Our ability to correlate *kyc* BGC expression within WMMB235 to the production of **1**, coupled with the realization that pathway-specific regulators often cluster within or proximal to BGCs,[37] inspired us to search the *kyc* cluster for regulatory gene candidates. This search revealed, among others, a *luxR*-type transcriptional regulator termed herein *kyc5*. In view of LuxR's well established role in QS in Gram-negative bacteria,[1,38,39] we posited that Kyc5 activation (via AHL exposure) may trigger keyicin production. Accordingly, we investigated the impact of established LuxR-selective ligands upon keyicin production. A library of 96 AHLs and related analogs (both natural products and synthetics) were screened for the ability to trigger keyicin production by monocultures of WMMB235.

A range of putative LuxR ligand concentrations were investigated, and even at the lowest concentration (1 nM), six compounds (Figure 2a) were found to activate keyicin

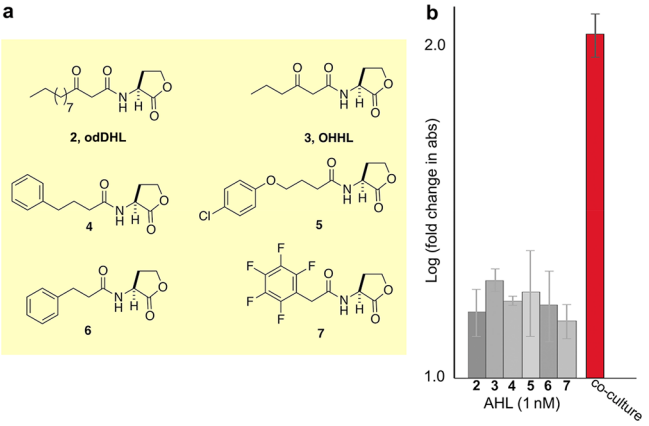

Figure 2. AHL inducers of keyicin. (a) Six out of 96 AHLs screened for *kyc* cluster activation and subsequent keyicin production: **2** and **3** are natural AHLs, whereas **4**–**7** are synthetic. (b) Increase in keyicin production shown as positive log fold change in the absorbance at 470 nm on treatment with AHLs compared to untreated monoculture; absorbance at 470 nm also enables detection of aglycone-containing precursors to **1**. Coculture with WMMA185 shown as positive control (red bar). AHLs **2** and **3** are the native LuxR signals in *P. aeruginosa* and *V. fischeri*, respectively.[3]

production as detected by increases in absorbance at 470 nm, which is diagnostic for production of the keyicin aglycone. The fold change in production of **1** was calculated by measuring the absorbance of cell supernatants of WMMB235 spiked with inducers (in DMSO) compared to its monoculture treated with DMSO alone. AHL-triggered keyicin production by WMMB235 was not as pronounced as in the WMMB235/WMMA185 coculture system (Figure 2b) indicating that production of **1** is subject to more than just one regulatory element. This, combined with the absence of any decipherable *luxI* homologues in the WMMA185 genome,[40] suggests that the LuxR pathway in the WMMA185/WMMB235 coculture system may respond to alternative (non-AHL) signals. Alternatively, *kyc* activation may be triggered by an altogether different mechanism. Although *luxI*/*luxR* are well studied in Gram-negative bacteria, it is only recently that these have been found not only in Gram-positive bacteria but also in other kingdom representatives.[41,42] In fact, several genomic studies across different species have found many QS-related *luxR* type genes that are unpaired to a cognate *luxI* to synthesize the signaling molecule and thus encode "orphan" LuxR receptors or "solos".[43,44] This supports our hypothesis that an "orphan" LuxR in *Micromonospora* sp. may be involved in interspecies

DOI: 10.1021/acschembio.9b00223
ACS Chem. Biol. 2019, 14, 1260–1270

communication by interacting with the small molecule signal from *Rhodococcus* sp. It is altogether possible that keyicin production may require pathways in addition to, or even instead of, LuxR. For instance, efficient production of pyocyanin, a phenazine virulence factor produced by *Pseudomonas aeruginosa* calls upon a total of three separate, but interwoven regulatory systems.[45] The results of Figure 2 may reflect a similar scenario in which LuxR-type signaling plays an important but not exclusive role in *kyc* cluster activation. In the absence of other clear and readily testable regulatory elements related to *kyc* activation, we sought to better understand the proteomics and transcriptomics of the WMMB235/WMMA185 coculture.

Isobaric Tagging Reveals Important Proteomic Profiles Unique to WMMB235/WMMA185 Coculture. We applied a quantitative proteomics approach to evaluate WMMB235/WMMA185 cocultures to identify unique elements of coculture that could be clearly correlated to *kyc* cluster activation and biosynthesis of **1**. Proteomics initiatives were carried out on 5-day long and 8-day long fermentations in order to most accurately capture protein levels. To reduce the complexity of samples subjected to proteomics, we employed a simulated coculture system wherein the supernatant of WMMA185 (5 d fermentation) was used as the WMMB235 growth medium. This enabled us to more confidently assign proteomic signatures to the keyicin producer and not *Rhodococcus* products. Established DiLeu tagging methods[46] allowed us to multiplex all samples and generate quantitative data on proteins of WMMB235 origin.

A marginal number (i.e., 12) of putatively biosynthetic proteins coded for by the *kyc* cluster (~49 based on *kyc orfs*) were identified from the 8-day fermentation of WMMB235 (Figure 3); these included four glycosyltransferases (GTs)

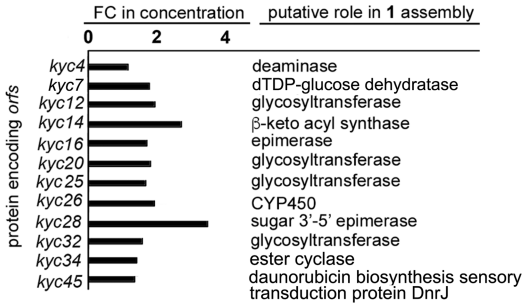

Figure 3. Summary of quantitative proteomics studies of WMMB235 fermented in WMMA185 supernatant (*Rhodococcus* cell free) for 8 d. FC, Fold change as compared to WMMB235 monoculture conditions. $N = 3$, $P < 0.05$.

(Kyc12, Kyc20, Kyc25, and Kyc32), all of which are significantly upregulated in coculture, as well as the putative dehydratase (Kyc7), β-keto acyl synthase (Kyc14), epimerase (Kyc16), cytochrome P_{450} (Kyc26), and dTDP-4-dehydrorhamnose 3,5-epimerase (Kyc28). The GTs Kyc12, Kyc20, and Kyc32 are all homologous to AknK, which is the GT responsible for adding the second and third 2-deoxy-L-fucose moieties during aclacinomycin biosynthesis (MIBiG, BGC0000191).[47] Kyc25, on the other hand, shares 61% identity with CosG, a GT known to transfer aminodeoxysugars like L-rhodosamine during biosynthesis of cosmomycin D (MIBiG, BGC0001074).[48] In depth sequence analyses for Kyc28 revealed 69% similarity to the sugar 3′-5′ epimerase SnogF (accession no. A0QSK5.1) involved in the deoxyhexose pathway required for nogalamycin assembly.[49] Interestingly, this protein was one of the few found in our initial proteomics study to be predominant in the coculture compared to the WMMB235 monoculture.[29] Additionally, Kyc26 was reported to have 42% protein identity with SnogN,[29] which in turn shares similarity with AknT (43%) and CosT (39%) and is also considered to be involved in the deoxyhexose pathway, especially in the biosynthesis of nogalamine.[50] The closest homologue to Kyc16 is a putative NDP-sugar 4-ketoreductase encoded within the versipelostatin gene cluster (MIBiG, BGC0001204). Importantly, Kyc14 with 65% identity with AknC, also from the aclacinomycin biosynthetic pathway, is the only *kyc orf* product found thus far that plays a role in the biosynthesis of the keyicin aglycone. Overall, four of the 12 proteins (33%) identified at the late 8 d fermentation are GTs suggesting that glycosylation likely takes place following aglycone assembly, that is, late in keyicin biosynthesis. As such, the GTs involved in keyicin production appear to function as true tailoring enzymes. Such a profile is consistent with other anthracycline biosynthetic studies where hydroxylated aglycone intermediates added exogenously to fermentation systems serve as efficient substrates for glycosylation.[51]

Coculture Dependent Proteomic Changes Correlate to *kyc* Cluster Metabolomics. The prominent changes in GT production found in coculture versus monoculture inspired us to investigate the prospect that keyicin analogs or precursors might be generated during coculture and other related keyicin-generating conditions but may have evaded detection. This hypothesis was further supported by the clear presence of many other compounds with distinct retention times in coculture extracts, all of which contained a chromophore with unique absorption at $\lambda = 470$ nm and MS/MS signals at $m/z = 550.1696$ and 586.1899 representative of the keyicin aglycone (Figure S4, Supporting Information). The relationship of these molecules with keyicin could be easily identified by subjecting the liquid chromatography tandem mass spectrometry (LC-MS/MS) analyses of coculture extracts collected over a fermentation period of 14 days to Global Natural Product Social (GNPS) Molecular Networking[52] and subsequent visualization by Cytoscape[53] (Figure 4). By tracking the node representative of keyicin (m/z 805.347), we identified the subcluster that contained the keyicin analogs and intermediates. On mapping the AUC (Area Under Curve) for each of the parent masses identified in the cluster at each time point, we discovered that many of these signals initially increased in intensity and then gradually subsided with time consistent with the biosynthetic progression leading ultimately to keyicin and away from incompletely glycosylated intermediates or precursors. For example, a doubly charged peak on the chromatogram corresponding to m/z values of 661.3050 and 645.7829 show a distinct temporal pattern. We propose that these signals represent differentially glycosylated analogs of keyicin. The m/z value of 645.7829 is consistent with decilonitrose,[29] the adduct resulting from the absence of keyicin's terminal 2-deoxy-fucose (S7, Figure 1). Additionally, the absence of both S3 and S7 (Figure 1) is likely reflected by the m/z signal at 661.305 (Figure S5, Supporting Information).

Having identified changes to the transcriptomic and proteomic profile as well as the players in keyicin production, and realizing that these changes likely invoke coculture-dependent changes that go beyond changes in *kyc* expression,

DOI: 10.1021/acschembio.9b00223
ACS Chem. Biol. 2019, 14, 1260−1270

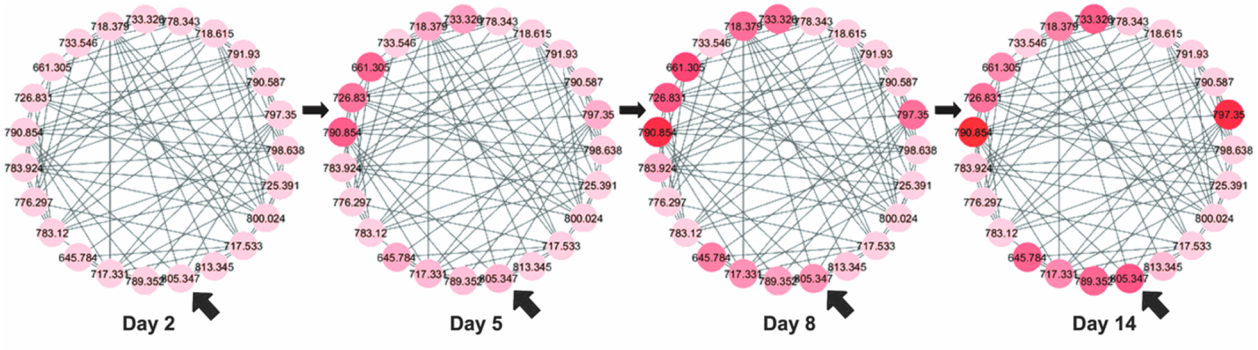

Figure 4. GNPS and Cytoscape visualization of keyicin analog masses (from LC-MS/MS of cocultured WMMB235) reflect varying extents of glycosylation over time (days 2, 5, 8, and 14). Continuous color mapping for each node in the network represents the relative concentrations of the species for which MS data is shown. Color intensities correlate to concentrations of each species for which MS data is acquired. The *m*/*z* signal for keyicin (805.347) is indicated at each time point with a thick diagonal arrow.

we next sought to investigate *kyc*-specific transcriptional changes as well as those of the whole WMMB235 genome.

Impacts of Coculture on the WMMB235 Genome Revealed by Transcriptomics. Transcriptomic evaluation of the *Micromonospora* sp. WMMB235 genome in WMMB235/WMMA185 cocultures dramatically expanded what we know about *kyc* activation as well as the modulation of other WMMB235 embedded BGCs. These efforts also provided clarity into how *Rhodococcus*-derived small molecule induction can be correlated to changes in protein expression and production and commensurate biosynthesis of **1**. Notably, transcriptomics analysis of the *kyc* cluster revealed that effectively all *orfs* within the cluster show some level of overexpression. Only *kyc4*, *5*, *30*, *31*, *39*−*42*, and *53* showed less than a 4-fold increase in expression relative to WMMB235 monoculture (Figure 5). Interestingly, *kyc30* and *kyc31*, both

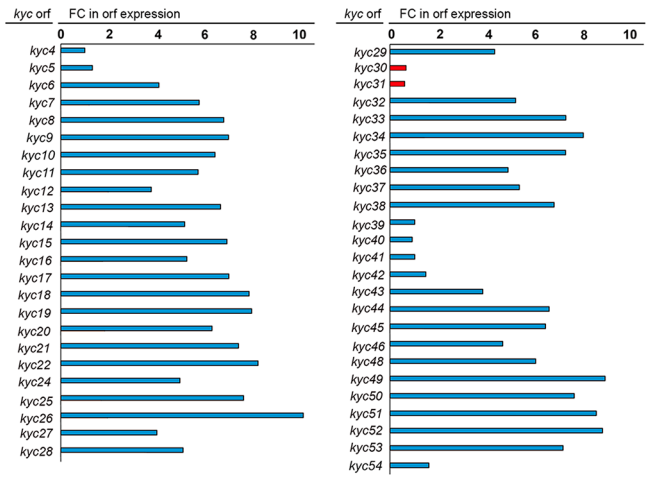

Figure 5. Summary of *kyc* cluster *orf* expression profiles in WMMB235/WMMA185 coculture compared to those generated in WMMB235 monoculture. Out of 49 *orfs* within the *kyc* cluster, only 6 undergo less than a 4-fold increase in expression and two (*kyc30*, *31* in red) appear to be suppressed in coculture. That these *orfs* appear to be dispersed at 3−4 different groupings within the *kyc* cluster suggests that *kyc* cluster regulation calls for more than just one global regulator. Beyond the earlier stated *orf*-to-function projections, a comprehensive listing of *kyc* genes and their putative roles in keyicin biosynthesis is provided in Table S3 of Supporting Information. FC, fold change. False Discovery Rate (*q*-value) for each gene expression change ≪ 0.01.

coding for transcriptionally suppressive regulators (Table S3, Supporting Information) were slightly suppressed under coculturing (FC < 1.0). With respect to *kyc* cluster-specific changes, it is clear that the overwhelming majority of *kyc* cluster elements in WMMB235 monoculture suffer from limited transcription relative to coculture. That coculture driven transcriptomic enhancements are so much more dramatic than those seen at the proteomics level suggests that the production of **1** in WMMB235 monoculture is most likely limited or bottlenecked at a transcriptional level.

The clustering of biosynthetic genes on bacterial chromosomes enables computational approaches to identifying sources of new natural products.[54] Although the biological logic for defining and identifying a BGC is conserved, different algorithms approach BGC prediction differently. AntiSmash v 3.0 data processing for the WMMB235 genome[34] revealed the presence of 50 putative BGCs, whereas PRISM processing of the same data set revealed the presence of 10 putative BGCs. The abundance of BGCs found by AntiSmash can be attributed to the low confidence/high novelty algorithm of ClusterFinder to identify BGCs. This probabilistic algorithm is optimized for detecting unknown types of gene clusters and consequently gives relatively high rates of false positives in the results.[15,33,54] As such, we restricted our transcriptomics analyses to only BGCs that resulted from PRISM; as expected, these same BGCs were also identified by AntiSmash processing of the WMMB235 genome.

In addition to their correlation of *kyc* cluster elements (i.e., transcripts and protein levels) to the production and structure of **1**, transcriptomics on the WMMB235 genome revealed that many other putative BGCs (annotated using PRISM) undergo transcriptomic changes in response to coculture with *Rhodococcus* sp. WMMA185. These include, as summarized in Table 1, several hybrid NRPS-type I PKS gene clusters (BGC4, 5, 6, 8), a type II PKS (BGC3), an AT-less type I PKS (BGC2), and clusters encoding a putative enediyne (BGC7) and lanthipeptide (BGC10). Impressively, of the 10 putative BGCs identified, nine are positively impacted by the presence of WMMA185 during fermentation, and of these, *kyc* was the dominantly impacted cluster (Figure 6). This transcriptomics finding is especially interesting since all 10 BGCs, except for *kyc* which has 79% similarity to aclacinomycin, have little similarity to known clusters in the MIBiG repository, making them orphan clusters (Table 1). Tentative mapping of BGC2−10 is shown in Figure 7, and prominent in these findings is the

DOI: 10.1021/acschembio.9b00223
ACS Chem. Biol. 2019, 14, 1260−1270

Table 1. BGCs Identified Within the *Micromonospora* sp. WMMB235 Genome as Annotated by PRISM[a]

BGC no.	cluster annotation	closest known homologous BGC[b]
1	keyicin	aclacinomycin[55] (72%) (BGC0000191)
2	AT-less PKS	leinamycin[56] (15%) (BGC0001101)
3	type II PKS	xantholipin[57] (16%) (BGC0000279)
4	NRPS-T1PKS	bleomycin[58] (12%) (BGC0000963)
5	NRPS-T1PKS	azicemicin[59] (13%) (BGC0000202)
6	NRPS-T1PKS	
7	enediyne	tiancimycin[60] (19%) (BGC0001378)
8	AHBA BGC	rifamycin[61] (35%) (BGC0000137)
9	T1PKS	chlorizidine A[62,63] (7%) (BGC0001172)
10	lanthipeptide	

[a]Assigned cluster numbers correlate to all subsequent tables and figures. [b]Values in parentheses correspond to percentatge of genes similar to those in the WMMB235 embedded cluster and MiBIG number, respectively.

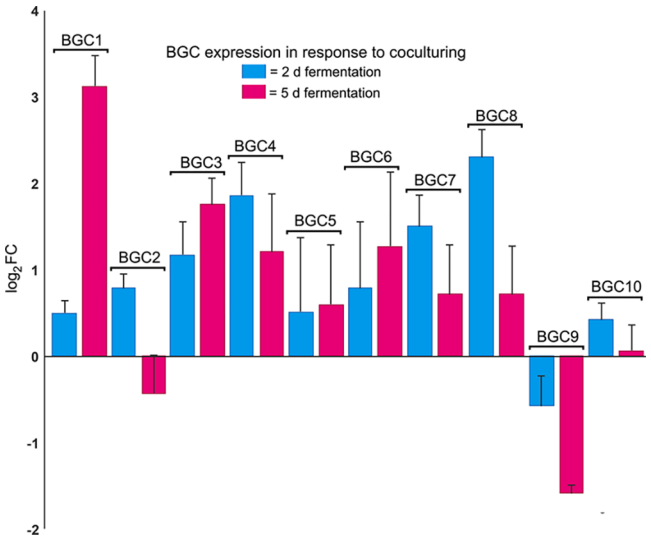

Figure 6. Global changes in BGC expression profiles in cocultured WMMB235 shown as logarithm of the fold change (FC) with base 2. The RPKMO over all the ORFs annotated by PRISM for each cluster were used to calculate the overall FCs. BGC numbers correlating to Table 1 are above each relevant bar, and expression profiles were obtained following 2 day (blue) or 5 day (purple) fermentations. N = 3.

presence of *luxR orfs* embedded within BGC3 and 8. These findings bolster our hypothesis that new chemical scaffolds are yet to be found in WMMB235 and that coculturing or its emulation (e.g., via LuxR activation with synthetic AHLs or WMMA185-derived LuxR agonists) may enable a host of new natural product discoveries.

Coculturing WMMB235 with WMMA185 appeared to impair transcription for only two BGCs within the WMMB235 genome, BGC2, a type I PKS−NRPS hybrid with a trans-acyltransferase (AT) domain, and BGC9, which is a type I PKS. The closest homologous cluster for BGC2 is that of leinamycin[56] (MIBiG, BGC0001101) with only 15% similarity. This cluster, in particular, is interesting as its expression is enhanced early on during coculturing but is then slightly repressed by day 5. Perhaps most interesting about this finding is that, of the BGC2 *orfs* suppressed in coculture at day 5, those involving transport are the most strongly represented. Though further studies await, we envision that diminished transporter production with respect to BGC2 may represent some form of defense by way of restricted extracellular access.

BGC9 is the smallest BGC identified of the 10 found in the WMMB235 genome and is a type I PKS with only 7% similarity to any known BGC, chlorizidine A (MIBiG, BGC0001172) (Table 1). For BGC2, eight genes had >1 log negative fold change on day 5 (Table S4, Supporting Information), which notably included all the transporter genes. For BGC9, *orf* downregulation was prominent and consistent over the full course of coculture fermentation. BGC9 suppression, as reflected in Figure 6 was dramatic relative to all other BGCs noted. A point-by-point assessment of specific *orfs* within BGC9 that were negatively impacted by coculturing is shown in Table S5 (Supporting Information). Unlike the BGC2 case, there is no one group or type of gene that is significantly downregulated although it is clear that elements of the PKS machinery for BGC9 are clearly impacted by coculturing. We posit that this may simply be a random event, or more enticingly, this may represent one means by which WMMB235 turns down production of a BGC9 encoded product. This may benefit the organism by allowing raw materials to be more wisely used given the competitive conditions of coculturing, or it may be a direct means of self-defense.

Transcriptomics of the WMMB235 genome made clear the ubiquity with which this organism appears to employ LuxR-based QS systems in embedded BGCs. BGC8 (Figures 6 and 7) was found to contain 184.203 kbp of information and to encode for a hybrid NRPS−type I PKS cluster with 22 modules and with 3-amino-5-hydroxy benzoic acid (AHBA) as a predicted substrate in one of the synthetase/ligase domains

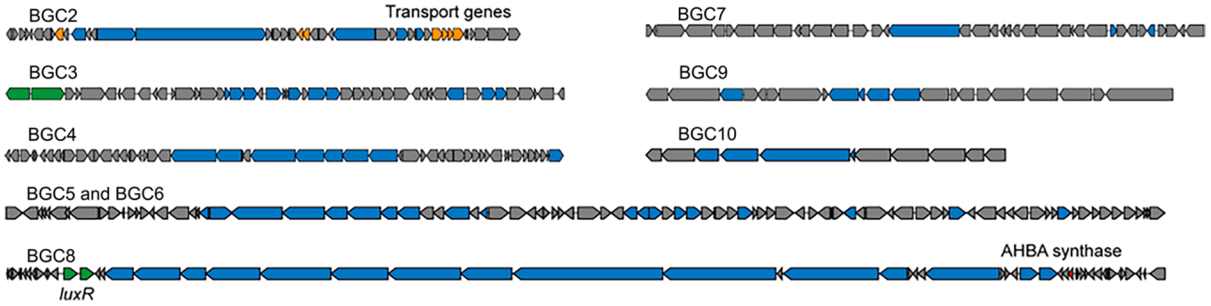

Figure 7. Early schematics of BGC2−10 (Table 1, Figure 6) from WMMB235 as annotated using both PRISM and AntiSmash. Blue ORFs indicate core biosynthetic operons. Transporter operons in BGC2 (yellow), *luxR* operons found in BGC3 and 8 (green), and AHBA synthase genes (red) in BGC8 are all highlighted.

DOI: 10.1021/acschembio.9b00223
ACS Chem. Biol. 2019, 14, 1260−1270

(Figure 7). A large group of natural products in the family of ansamycins, mitomycins, and saliniketals utilize AHBA as a precursor,[64] although BGC8 is only 35% similar to the closest ansamycin BGC of rifamycin (MIBiG, BGC0000137). More telling about BGC8 is that, in contrast to *kyc*, it contains two *luxR* genes, both of which code for products with 36% similarity to GdmRII (ABI93788.1). GdmRI and GdmRII are known homologues of LuxR proteins that positively regulate the production of geldanamycin in *Streptomyces hygroscopicus* 17997.[65] This suggests that BGC8, in addition to *kyc*, may also be regulated using small molecule inducers. Notably, although BGC8 is an orphan cluster, similar clusters are present in other *Micromonospora* spp. such as *Micromonospora* sp. strain B006.[66] Finally, it warrants noting that, besides *kyc* and BGC8, these transcriptomics studies revealed the presence of two *luxR* genes within the type II PKS-encoding BGC3. It is clear that WMMB235 embedded BGCs harbor the potential to exploit LuxR-based QS pathways, presumably to regulate secondary metabolism in response to assorted cellular challenges.

Changes in Global KEGG Categorization. Analysis of transcriptomics and genomics data for WMMB235 monocultures versus WMMB235/WMMA185 cocultures using Kyoto Encyclopedia of Genes & Genomes (KEGG) software revealed further insight into changes that occur within WMMB235 during coculture and that likely have a bearing on the expression of the *kyc* and other BGCs and their products.

As reflected in Figure 8, significant shifts are seen based on the duration of fermentation (2 vs 5 days) as well as the presence or absence of WMMA185. Particularly interesting are the significant increases in carbohydrate metabolism, energy metabolism, and metabolism of terpenoids and polyketides observed in coculture at day 5 (Figure 8, lane 4). Perhaps also noteworthy is the apparent reduction in translational capacity at day 5 in coculture relative to WMMB235 monoculture. Notably, these changes are reflective of altered gene expression with respect to the whole WMMB235 genome and most certainly encompass changes that have a bearing on keyicin production. Indeed, it is likely that the results of these KEGG studies can be understood, in part, by the transcriptomics changes depicted in Figure 6. In essence, the results shown in Figures 6 and 8 are clearly related; whereas Figure 6 conveys *kyc* cluster specific changes, Figure 8 provides a more global view of how WMMB235 genome readout and processing changes in response to coculturing with WMMA185.

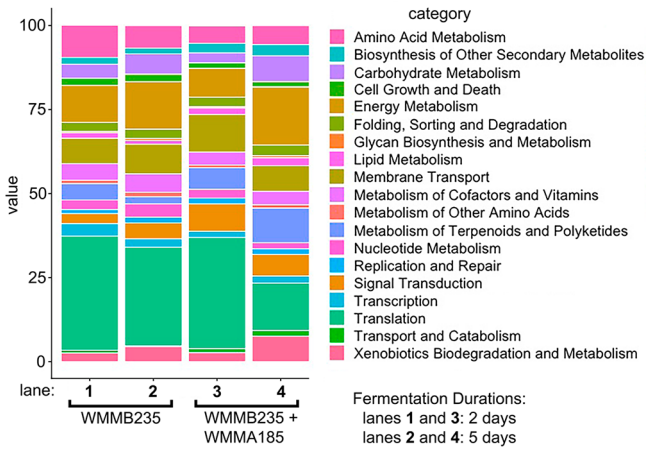

Figure 8. Summary of KEGG mapping for WMMB235 monoculture versus coculture with WMMA185. Lane contents are shown by combination of bracketing and lane coding below the categories listing. Coculturing and duration of fermentations both impact gene expression within WMMB235. Categories of function not abundant enough to depict graphically involved cell communication, cell motility, and signal molecules and interaction. All other categories are depicted in one or more of lanes 1−4.

Future Directions. In sum, the ability to track transcriptomic and proteomic information in relation to WMMB235/WMMA185 coculture and subsequent keyicin production sheds significant insight into the activation of *kyc*, an otherwise silent BGC. That keyicin production is also triggered by a panel of established QS ligands for LuxR supports the involvement of a LuxR-based system in dictating whether WMMB235 can generate keyicin. The correlation of these omics data, QS results, and keyicin biosynthesis support the notion that, by comparing BGC host transcriptomes, proteomes, and metabolomes between monoculture and coculture scenarios, the identification of biosynthetic bottlenecks in monoculture as well as strategies by which to circumvent or overcome such bottlenecks is readily feasible. Our findings suggest that monocultured WMMB235 suffers from one or more transcriptionally based bottlenecks with respect to keyicin assembly. This logic is apparent when comparing transcriptomic and proteomic profiles of WMMB235 monoculture versus WMMB235/WMMA185 (or related) systems. At the same time, delineating possible regulatory differences in mono- and cocultures is envisioned to expand our understanding of microbial combinations able to activate cryptic BGCs.

METHODS

Transcriptomics. WMMA185 and WMMB235 were grown in monoculture and coculture in triplicate as described previously.[29] Aliquots of 1.5 mL were taken from day 2 and day 5 for each sample and frozen at −80 °C. At the end of the experiment, the samples were thawed and centrifuged to collect the cell mass. Cells were lysed by freezing the samples in liquid nitrogen and mechanically breaking them in a mortar and pestle. The RNA was extracted using RNAeasy Plus Mini Kit according to the manufacturer's instructions (Supporting Information) and sent to UW—Madison Biotech Center for sequencing, quality control, and read mapping. RNAs used to generate transcriptomics data originated from mono- and coculture fermentations whose metabolomics analyses reproducibly adhered to expectation. Briefly, the rRNA was depleted using Ribo-Zero rRNA removal kit (Epicenter), and TruSeq Total RNA v2 Illumina library was prepared. The samples were subjected to Illumina HiSeq 2500 at 1 × 100 bp read length. Extensive QC was conducted on the resultant sequencing data (Supporting Information) and showed high quality reads. The filtered RNA sequences were aligned with Bowtie 2[67] to contigs in the WMMB235 assembly using the end-to-end alignment options "-very-sensitive -no-discordant -no-unal". The WMMB235 assembly was annotated with Prokka[68] and normalized reads per kbp of gene per million (RPKM) reads was calculated for each ORF annotated. Differential gene expression for RNA-Seq results from day 5 were analyzed using EdgeR with GLM after alignment of each of the two species, WMMB235 and WMMA185, to a "hybrid" genome created from both. Functional Kyoto Encyclopedia of Genes and Genomes (KEGG) categories were assigned to the predicted protein sequences for WMMB235 using MEGAN[69] with previously described methods.[70] KEGG trees were uncollapsed two levels in MEGAN, and all assignments except for "organismal systems" and "human diseases" were exported to a csv file (with the columns "read name" and "KEGG name"). Calculated RPKM values and the MEGAN csv table

DOI: 10.1021/acschembio.9b00223
ACS Chem. Biol. 2019, 14, 1260−1270

were used to calculate proportions of the WMMB235 transcriptome that corresponded to each KEGG category.

Proteomics. WMMA185 was grown in 100 mL culture in triplicate in ASW-D media for a period of 5 days. The content of each of these culture flasks was then vacuum filtered through 0.2 μm PES filters (Thermo Scientific Nalgene Rapid-Flow Sterile Disposable Filter Units) and transferred to three new flasks. These were inoculated with WMMB235 and incubated in a shaker. Aliquots after 5 and 8 days of culture were taken and frozen in −80 °C freezer. The cells were lysed using a lysis buffer (10 mL) containing 8 M urea (4.8048 g), 50 mM Tris Base (60.57 mg), 5 mM $CaCl_2$ (5.5 mg), 20 mM NaCl (17.5 mg), 1 EDTA-free Roche protease inhibitor tablet (11836170001), 1 Roche PhosSTOP phosphatase inhibitor tablet (04906845001), and 25 μL of 12.1 N HCl (to make pH ≈ 8). To 100 μL of cell lysate, 500 μL of lysis buffer was added. This was vortexed and subsequently sonicated with a probe sonicator by applying 12 15 s pulses at 50% amplitude, each followed by a 30 s rest period. Care was taken to ensure the sample was kept cold. The sample then underwent trypsin digestion using 2 μg of trypsin and incubating for 18 h at 37 °C. Subsequently, the samples were labeled using Dileu (Supporting Information), following a published protocol.[46] Labeled day 5 or day 8 bacterial peptides were combined as 6-plex mixtures. The mixtures were purified by strong cation exchange liquid chromatography (SCX LC) with a PolySULFOETHYL A column (200 mm × 2.1 mm, 5 μm, 300 Å, PolyLC, Columbia, MD). Eluates containing labeled peptides were collected with an FC-4 fraction collector (Rainin Dynamax) and dried under vacuum. Samples were then fractionated with a Kinetex C18 column (5 μm, 100 Å, Phenomenex, Torrance, CA) at pH = 10 into 8 fractions. Each fraction was dried under vacuum several times.

Peptides in each fraction was reconstituted in 0.1% formic acid (FA) and subjected to reversed phase LC-MS/MS analysis with an Orbitrap Fusion Lumos Tribrid mass spectrometer (Thermo Fisher Scientific, San Jose, CA) interfaced with a Dionex Ultimate 3000 UPLC system (Thermo Fisher Scientific, San Jose, CA). Peptides were loaded onto a 75 μm inner diameter microcapillary column custom-packed with 15 cm of bridged ethylene hybrid C18 particles (1.7 μm, 130 Å, Waters). Labeled peptides were separated with a 120 min gradient from 3% to 30% ACN with 0.1% FA, followed by 10 min to 75% ACN, and then 10 min to 95% ACN. After that, the column was equilibrated at 3% ACN for 15 min to prepare for the next injection. Survey scans of peptide precursors from 350 to 1500 m/z were performed at a resolving power of 60000 and an AGC target of 2×10^5 with a maximum injection time of 100 ms. The top 20 intense precursor ions were selected and subjected to the HCD fragmentation at a normalized collision energy of 27% followed by tandem MS acquisition at a resolving power of 30000 and an AGC target of 5×10^4, with a maximum injection time of 54 ms and a lower mass limit of 110 m/z. Precursors were subjected to a dynamic exclusion of 45 s with a 10 ppm mass tolerance.

Raw files were processed with PEAKS Studio (Bioinformatics Solutions Inc., Waterloo, ON, Canada). Trypsin was selected as the enzyme with the maximum two missed cleavages. Spectra were first annotated by de Novo sequencing then searched by PEAKS 7.0 against a transcriptome predicted protein database for WMB235, where the parent mass error tolerance was set to be 25.0 ppm and fragment mass tolerance was 0.3 Da. Fixed modifications included DiLeu labels on peptide N-termini and lysine residues (+145.12801 Da) and carbamidomethylation on cysteine residues (+57.02146 Da). Dynamic modifications included oxidation of methionine residues (+15.99492 Da) and deamidation of asparagine and glutamine residues (+0.98402 Da). Quantitation was performed with a reporter ion integration tolerance of 20 ppm with the peptide score threshold of 20.0. Protein quantitative ratios were calculated using unique peptides. Reporter ion ratios for protein groups were exported to Excel workbook, and Student t test was performed with biological triplicates. Proteins that had >50% fold change and $p < 0.05$ were filtered as significantly changed.

Metabolomics. WMMB235 and WMMA185 cultures grown in triplicate for transcriptomics analysis were allowed to grow for 14 days and were also used to collect aliquots of 1.5 mL for metabolomic analyses. The collected samples were processed using solid phase extraction and analyzed using UHPLC/UV/qTOF-HRESI-MS/MS.[29,71] Briefly, solubilized extracts in 10:1 H_2O/MeOH were subjected to automated SPE using a Gilson GX-271 liquid handling system. Briefly, extracts were loaded onto EVOLUTE ABN SPE cartridges (25 mg absorbent mass, 1 mL reservoir volume; Biotage, S4 Charlotte, NC), and eluted with MeOH (500 μL) directly into an LC/MS-certified vial. LC/MS data were acquired using a Bruker MaXis ESI-qTOF mass spectrometer (Bruker, Billerica, MA) coupled with a Waters Acquity UPLC system (Waters, Milford, MA) operated by Bruker Hystar software. Chromatographic separations were achieved with a gradient of MeOH and H_2O (containing 0.1% formic acid) on an RP C-18 column (Phenomenex Kinetex 2.6 μm, 2.1 mm × 100 mm; Phenomenex, Torrance, CA) at a flow rate of 0.3 mL/min. The method was as follows: 1−12 min (10%−97% MeOH in H_2O) and 12−14 min (97% MeOH). Full scan mass spectra (m/z 150−1550) were measured in positive ESI mode. The mass spectrometer was operated using the following parameters: capillary, 4.5 kV; nebulizer pressure, 1.2 bar; dry gas flow, 8.0 L/min; dry gas temperature, 205 °C; scan rate, 2 Hz. Tune mix (ESI-L low concentration; Agilent, Santa Clara, CA) was introduced through a divert valve at the end of each chromatographic run for automated internal calibration. The full scan spectra were followed by MS/MS spectra acquisition at variable scan speed ranging from 0.5 to 2 Hz. CID energy varied linearly, 30, 25, and 20 eV for 500 m/z, 50, 40, and 35 eV for 1000 m/z, and 70, 50, and 45 eV for 2000 m/z for charge states of 1, 2, and 3, respectively. The precursor list was set to exclude precursor ions for 1.00 min after 3 spectra with the same precursor ion have been acquired. Bruker DataAnalysis 4.2 software was used for analysis of chromatograms and to convert MS/MS data from d files to mzXML. These files were then uploaded to the Mass Spectrometry Interactive Virtual Environment (MassIVE) server (https://massive.ucsd.edu/ProteoSAFe/static/massive.jsp) and networked using the GNPS pipeline.[52] Parent ions with at least three fragments were considered in the network. A cosine similarity score of 0.7 for the fragmentation spectra was used. The resulting networks were visualized using Cytoscape 3.5.1 (www.cytoscape.org/cy3.html).[53] The network containing parent ions representative of keyicin (m/z 805.347 and 797.35) was extracted and further analyzed. For each of the ions in the network, the AUC was calculated from the corresponding LC-MS data using the integrate method in the DataAnalysis software. These values were fed back into Cytoscape to color the nodes using continuous mapping color for each day.

AHL Induction Assay. Seed cultures of WMMB235 were grown in five portions of 10 mL of ASW-D media (Supporting Information).[3,72,73] After 3 days of culture, polypropylene square 96-deep well microplates (Enzyscreen, The Netherlands) containing 500 μL of ASW-D were inoculated with 15 μL of WMMB235, and 5 μL of AHL dissolved in DMSO at five concentrations was added to it in triplicate. Monocultures and coculture controls were also inoculated as described before.[71] The culture plates were incubated at 30 °C for 14 days and shaken at 300 rpm. Subsequently, the plates were centrifuged at 3000 rpm for 20 min (Eppendorf Centrifuge 5810R), the supernatants were transferred to a Corning Clear Polystyrene 96-Well Microplate, and the absorption at 470 nm was recorded using a BioTek Synergy microplate reader.

■ ASSOCIATED CONTENT

Supporting Information

The Supporting Information is available free of charge on the ACS Publications website at DOI: 10.1021/acschembio.9b00223.

Parameters for AntiSmash and Transcriptomics studies as well as a summary of RNA concentrations yielded from RNAeasy Plus Mini Kit extractions, a listing of DiLeu reporter tags used to label each sample in the multiplex analyses, and schematics showing coculture

DOI: 10.1021/acschembio.9b00223
ACS Chem. Biol. 2019, 14, 1260−1270

interactions leading to *kyc* activation, sample quality control report for RNASeq reads, strategy for DiLeu tagging in proteomics, MS/MS data sets and temporal changes to keyicin production (PDF)

AUTHOR INFORMATION

Corresponding Author

*T.S.B. E-mail: tim.bugni@wisc.edu.

ORCID

Ian Miller: 0000-0001-5084-9035
Lingjun Li: 0000-0003-0056-3869
Helen E. Blackwell: 0000-0003-4261-8194
Tim S. Bugni: 0000-0002-4502-3084

Notes

The authors declare no competing financial interest.

ACKNOWLEDGMENTS

This work was supported by funding from the University of Wisconsin—Madison School of Pharmacy and from the University of Wisconsin Institute for Clinical and Translational Research funded through NIH/NCATS UL1TR000427. This work was also funded by the NIH through the administration of NIGMS Grants R01GM104192 (T.S.B.), R01GM109403 (H.E.B), and NIDDK R01DK071801 (to L.L.). We thank the Analytical Instrumentation Center at the University of Wisconsin—Madison for the facilities to acquire spectroscopic data. Orbitrap instruments were purchased through the support of an NIH shared instrument grant (NIH-NCRR S10RR029531 to L.L.) and the Office of the Vice Chancellor for Research and Graduate Education at the University of Wisconsin—Madison. L.L. acknowledges a Vilas Distinguished Achievement Professorship and a Janis Apinis Professorship with funding provided by the Wisconsin Alumni Research Foundation and University of Wisconsin—Madison School of Pharmacy. I.M. was supported in part by a predoctoral fellowship from the American Foundation for Pharmaceutical Education. M.J.S. was supported in part by the National Institute of General Medical Sciences of the NIH under Award Number T32 GM008349 and by the National Science Foundation Graduate Research Fellowship Program under Grant No. DGE-1747503. Any opinions, findings, and conclusions or recommendations expressed in this material are those of the authors and do not necessarily reflect the views of the National Science Foundation.

REFERENCES

(1) Bassler, B. L. (1999) How Bacteria Talk to Each Other: Regulation of Gene Expression by Quorum Sensing. *Curr. Opin. Microbiol. 2*, 582−587.

(2) Whiteley, M., Diggle, S. P., and Greenberg, E. P. (2017) Progress in and Promise of Bacterial Quorum Sensing Research. *Nature 551*, 313−320.

(3) Welsh, M. A., and Blackwell, H. E. (2016) Chemical Probes of Quorum Sensing: From Compound Development to Biological Discovery. *FEMS Microbiol. Rev. 40*, 774−794.

(4) Papenfort, K., Silpe, J. E., Schramma, K. R., Cong, J. P., Seyedsayamdost, M. R., and Bassler, B. L. (2017) A Vibrio Cholerae Autoinducer−Receptor Pair That Controls Biofilm Formation. *Nat. Chem. Biol. 13*, 551−557.

(5) Rutherford, S. T., and Bassler, B. L. (2012) Bacterial Quorum Sensing: Its Role in Virulence and Possibilities for Its Control. *Cold Spring Harbor Perspect. Med. 2*, a012427.

(6) Rasko, D. A., and Sperandio, V. (2010) Anti-Virulence Strategies to Combat Bacteria-Mediated Disease. *Nat. Rev. Drug Discovery 9*, 117−128.

(7) Njoroge, J., and Sperandio, V. (2009) Jamming Bacterial Communication: New Approaches for the Treatment of Infectious Diseases. *EMBO Mol. Med. 1*, 201−210.

(8) Ishida, K., Lincke, T., Behnken, S., and Hertweck, C. (2010) Induced Biosynthesis of Cryptic Polyketide Metabolites in a *Burkholderia Thailandensis* Quorum Sensing Mutant. *J. Am. Chem. Soc. 132*, 13966−13968.

(9) Mao, D., Bushin, L. B., Moon, K., Wu, Y., and Seyedsayamdost, M. R. (2017) Discovery of ScmR as a Global Regulator of Secondary Metabolism and Virulence in Burkholderia Thailandensis E264. *Proc. Natl. Acad. Sci. U. S. A. 114*, E2920−E2928.

(10) Majerczyk, C., Brittnacher, M., Jacobs, M., Armour, C. D., Radey, M., Schneider, E., Phattarasokul, S., Bunt, R., and Greenberg, E. P. (2014) Global Analysis of the Burkholderia Thailandensis Quorum Sensing-Controlled Regulon. *J. Bacteriol. 196*, 1412−1424.

(11) Schuster, M., Joseph Sexton, D., Diggle, S. P., and Peter Greenberg, E. (2013) Acyl-Homoserine Lactone Quorum Sensing: From Evolution to Application. *Annu. Rev. Microbiol. 67*, 43−63.

(12) Campbell, J., Lin, Q., Geske, G. D., and Blackwell, H. E. (2009) New and Unexpected Insights into the Modulation of LuxR-Type Quorum Sensing by Cyclic Dipeptides. *ACS Chem. Biol. 4*, 1051−1059.

(13) Stacy, D. M., Welsh, M. A., Rather, P. N., and Blackwell, H. E. (2012) Attenuation of Quorum Sensing in the Pathogen *Acinetobacter Baumannii* Using Non-Native *N* -Acyl Homoserine Lactones. *ACS Chem. Biol. 7*, 1719−1728.

(14) Moore, J. D., Rossi, F. M., Welsh, M. A., Nyffeler, K. E., and Blackwell, H. E. (2015) A Comparative Analysis of Synthetic Quorum Sensing Modulators in *Pseudomonas Aeruginosa* : New Insights into Mechanism, Active Efflux Susceptibility, Phenotypic Response, and Next-Generation Ligand Design. *J. Am. Chem. Soc. 137*, 14626−14639.

(15) Cimermancic, P., Medema, M. H., Claesen, J., Kurita, K., Wieland Brown, L. C., Mavrommatis, K., Pati, A., Godfrey, P. A., Koehrsen, M., Clardy, J., Birren, B. W., Takano, E., Sali, A., Linington, R. G., and Fischbach, M. A. (2014) Insights into Secondary Metabolism from a Global Analysis of Prokaryotic Biosynthetic Gene Clusters. *Cell 158*, 412−421.

(16) Amos, G. C. A., Awakawa, T., Tuttle, R. N., Letzel, A.-C., Kim, M. C., Kudo, Y., Fenical, W., Moore, B. S., and Jensen, P. R. (2017) Comparative Transcriptomics as a Guide to Natural Product Discovery and Biosynthetic Gene Cluster Functionality. *Proc. Natl. Acad. Sci. U. S. A. 114*, E11121−E11130.

(17) Medema, M. H., Kottmann, R., Yilmaz, P., Cummings, M., Biggins, J. B., Blin, K., de Bruijn, I., Chooi, Y. H., Claesen, J., Coates, R. C., Cruz-Morales, P., Duddela, S., Düsterhus, S., Edwards, D. J., Fewer, D. P., Garg, N., Geiger, C., Gomez-Escribano, J. P., Greule, A., Hadjithomas, M., Haines, A. S., Helfrich, E. J., Hillwig, M. L., Ishida, K., Jones, A. C., Jones, C. S., Jungmann, K., Kegler, C., Kim, H. U., Kötter, P., Krug, D., Masschelein, J., Melnik, A. V., Mantovani, S. M., Monroe, E. A., Moore, M., Moss, N., Nützmann, H. W., Pan, G., Pati, A., Petras, D., Reen, F. J., Rosconi, F., Rui, Z., Tian, Z., Tobias, N. J., Tsunematsu, Y., Wiemann, P., Wyckoff, E., Yan, X., Yim, G., Yu, F., Xie, Y., Aigle, B., Apel, A. K., Balibar, C. J., Balskus, E. P., Barona-Gómez, F., Bechthold, A., Bode, H. B., Borriss, R., Brady, S. F., Brakhage, A. A., Caffrey, P., Cheng, Y. Q., Clardy, J., Cox, R. J., De Mot, R., Donadio, S., Donia, M. S., van der Donk, W. A., Dorrestein, P. C., Doyle, S., Driessen, A. J., Ehling-Schulz, M., Entian, K. D., Fischbach, M. A., Gerwick, L., Gerwick, W. H., Gross, H., Gust, B., Hertweck, C., Höfte, M., Jensen, S. E., Ju, J., Katz, L., Kaysser, L., Klassen, J. L., Keller, N. P., Kormanec, J., Kuipers, O. P., Kuzuyama, T., Kyrpides, N. C., Kwon, H. J., Lautru, S., Lavigne, R., Lee, C. Y., Linquan, B., Liu, X., Liu, W., Luzhetskyy, A., Mahmud, T., Mast, Y., Méndez, C., Metsä-Ketelä, M., Micklefield, J., Mitchell, D. A., Moore, B. S., Moreira, L. M., Müller, R., Neilan, B. A., Nett, M., Nielsen, J., O'Gara, F., Oikawa, H., Osbourn, A., Osburne, M. S., Ostash, B.,

DOI: 10.1021/acschembio.9b00223
ACS Chem. Biol. 2019, 14, 1260−1270

Payne, S. M., Pernodet, J. L., Petricek, M., Piel, J., Ploux, O., Raaijmakers, J. M., Salas, J. A., Schmitt, E. K., Scott, B., Seipke, R. F., Shen, B., Sherman, D. H., Sivonen, K., Smanski, M. J., Sosio, M., Stegmann, E., Süssmuth, R. D., Tahlan, K., Thomas, C. M., Tang, Y., Truman, A. W., Viaud, M., Walton, J. D., Walsh, C. T., Weber, T., van Wezel, G. P., Wilkinson, B., Willey, J. M., Wohlleben, W., Wright, G. D., Ziemert, N., Zhang, C., Zotchev, S. B., Breitling, R., Takano, E., and Glöckner, F. O. (2015) Minimum Information about a Biosynthetic Gene Cluster. *Nat. Chem. Biol. 11*, 625−631.

(18) Udwary, D. W., Zeigler, L., Asolkar, R. N., Singan, V., Lapidus, A., Fenical, W., Jensen, P. R., and Moore, B. S. (2007) Genome Sequencing Reveals Complex Secondary Metabolome in the Marine Actinomycete Salinispora Tropica. *Proc. Natl. Acad. Sci. U. S. A. 104*, 10376−10381.

(19) Fenical, W., and Jensen, P. R. (2006) Developing a New Resource for Drug Discovery: Marine Actinomycete Bacteria. *Nat. Chem. Biol. 2*, 666−673.

(20) Abdelmohsen, U. R., Grkovic, T., Balasubramanian, S., Kamel, M. S., Quinn, R. J., and Hentschel, U. (2015) Elicitation of Secondary Metabolism in Actinomycetes. *Biotechnol. Adv. 33*, 798−811.

(21) Gross, H. (2007) Strategies to Unravel the Function of Orphan Biosynthesis Pathways: Recent Examples and Future Prospects. *Appl. Microbiol. Biotechnol. 75*, 267−277.

(22) Scherlach, K., and Hertweck, C. (2009) Triggering Cryptic Natural Product Biosynthesis in Microorganisms. *Org. Biomol. Chem. 7*, 1753−1760.

(23) Bentley, S. D., Chater, K. F., Cerdeño-Tárraga, A. M., Challis, G. L., Thomson, N. R., James, K. D., Harris, D. E., Quail, M. A., Kieser, H., Harper, D., Bateman, A., Brown, S., Chandra, G., Chen, C. W., Collins, M., Cronin, A., Fraser, A., Goble, A., Hidalgo, J., Hornsby, T., Howarth, S., Huang, C. H., Kieser, T., Larke, L., Murphy, L., Oliver, K., O'Neil, S., Rabbinowitsch, E., Rajandream, M. A., Rutherford, K., Rutter, S., Seeger, K., Saunders, D., Sharp, S., Squares, R., Squares, S., Taylor, K., Warren, T., Wietzorrek, A., Woodward, J., Barrell, B. G., Parkhill, J., and Hopwood, D. A. (2002) Complete Genome Sequence of the Model Actinomycete *Streptomyces Coelicolor* A3(2). *Nature 417*, 141−147.

(24) Rateb, M. E., Hallyburton, I., Houssen, W. E., Bull, A. T., Goodfellow, M., Santhanam, R., Jaspars, M., and Ebel, R. (2013) Induction of Diverse Secondary Metabolites in *Aspergillus Fumigatus* by Microbial Co-Culture. *RSC Adv. 3*, 14444−14450.

(25) Bertrand, S., Bohni, N., Schnee, S., Schumpp, O., Gindro, K., and Wolfender, J.-L. (2014) Metabolite Induction *via* Microorganism Co-Culture: A Potential Way to Enhance Chemical Diversity for Drug Discovery. *Biotechnol. Adv. 32*, 1180−1204.

(26) Kurosawa, K., Ghiviriga, I., Sambandan, T. G., Lessard, P. A., Barbara, J. E., Rha, C., and Sinskey, A. J. (2008) Rhodostreptomycins, Antibiotics Biosynthesized Following Horizontal Gene Transfer from Streptomyces Padanus to *Rhodococcus Fascians*. *J. Am. Chem. Soc. 130*, 1126−1127.

(27) Cueto, M., Jensen, P. R., Kauffman, C., Fenical, W., Lobkovsky, E., and Clardy, J. (2001) Pestalone, a New Antibiotic Produced by a Marine Fungus in Response to Bacterial Challenge. *J. Nat. Prod. 64*, 1444−1446.

(28) Pishchany, G., Mevers, E., Ndousse-Fetter, S., Horvath, D. J., Paludo, C. R., Silva-Junior, E. A., Koren, S., Skaar, E. P., Clardy, J., and Kolter, R. (2018) *Amycomicin* Is a Potent and Specific Antibiotic Discovered with a Targeted Interaction Screen. *Proc. Natl. Acad. Sci. U. S. A. 115*, 10124−10129.

(29) Adnani, N., Chevrette, M. G., Adibhatla, S. N., Zhang, F., Yu, Q., Braun, D. R., Nelson, J., Simpkins, S. W., McDonald, B. R., Myers, C. L., Piotrowski, J. S., Thompson, C. J., Currie, C. R., Li, L., Rajski, S. R., and Bugni, T. S. (2017) Coculture of Marine Invertebrate-Associated Bacteria and Interdisciplinary Technologies Enable Biosynthesis and Discovery of a New Antibiotic, Keyicin. *ACS Chem. Biol. 12*, 3093−3102.

(30) Skinnider, M. A., Dejong, C. A., Rees, P. N., Johnston, C. W., Li, H., Webster, A. L. H., Wyatt, M. A., and Magarvey, N. A. (2015) Genomes to Natural Products PRediction Informatics for Secondary Metabolomes (PRISM). *Nucleic Acids Res. 43*, 9645−9662.

(31) Medema, M. H., Blin, K., Cimermancic, P., De Jager, V., Zakrzewski, P., Fischbach, M. A., Weber, T., Takano, E., and Breitling, R. (2011) AntiSMASH: Rapid Identification, Annotation and Analysis of Secondary Metabolite Biosynthesis Gene Clusters in Bacterial and Fungal Genome Sequences. *Nucleic Acids Res. 39*, W339−346.

(32) Blin, K., Medema, M. H., Kazempour, D., Fischbach, M. A., Breitling, R., Takano, E., and Weber, T. (2013) AntiSMASH 2.0–a Versatile Platform for Genome Mining of Secondary Metabolite Producers. *Nucleic Acids Res. 41*, W204−W212.

(33) Weber, T., Blin, K., Duddela, S., Krug, D., Kim, H. U., Bruccoleri, R., Lee, S. Y., Fischbach, M. A., Müller, R., Wohlleben, W., Breitling, R., Takano, E., and Medema, M. H. (2015) AntiSMASH 3.0—a Comprehensive Resource for the Genome Mining of Biosynthetic Gene Clusters. *Nucleic Acids Res. 43*, W237−W243.

(34) Adnani, N., Braun, D. R., Mcdonald, B. R., Chevrette, M. G., Currie, C. R., and Bugni, T. S. (2017) Draft Genome Sequence of Micromonospora Sp. Strain WMMB235, a Marine Ascidian-Associated Bacterium. *Genome Announce 5*, e01369-16.

(35) Mandlik, A., Livny, J., Robins, W. P., Ritchie, J. M., Mekalanos, J. J., and Waldor, M. K. (2011) RNA-Seq-Based Monitoring of Infection-Linked Changes in Vibrio Cholerae Gene Expression. *Cell Host Microbe 10*, 165−174.

(36) Robinson, M. D., McCarthy, D. J., and Smyth, G. K. (2010) edgeR: A Bioconductor Package for Differential Expression Analysis of Digital Gene Expression Data. *Bioinformatics 26*, 139−140.

(37) Bibb, M. J. (2005) Regulation of Secondary Metabolism in Streptomycetes. *Curr. Opin. Microbiol. 8*, 208−215.

(38) Waters, C. M., and Bassler, B. L. (2005) Quorum Sensing : Communication in Bacteria. *Annu. Rev. Cell Dev. Biol. 21*, 319−346.

(39) Gerdt, J. P., Wittenwyler, D. M., Combs, J. B., Boursier, M. E., Brummond, J. W., Xu, H., and Blackwell, H. E. (2017) Chemical Interrogation of LuxR-Type Quorum Sensing Receptors Reveals New Insights into Receptor Selectivity and the Potential for Interspecies Bacterial Signaling. *ACS Chem. Biol. 12*, 2457−2464.

(40) Adnani, N., Braun, D. R., McDonald, B. R., Chevrette, M. G., Currie, C. R., and Bugni, T. S. (2016) Complete Genome Sequence of Rhodococcus Sp. Strain WMMA185, a Marine Sponge-Associated Bacterium. *Genome Announc 4*, e01406-16.

(41) Polkade, A. V., Mantri, S. S., Patwekar, U. J., and Jangid, K. (2016) Quorum Sensing: An Under-Explored Phenomenon in the Phylum Actinobacteria. *Front. Microbiol. 7*, 131.

(42) Santos, C. L., Correia-Neves, M., Moradas-Ferreira, P., and Mendes, M. V. (2012) A Walk into the LuxR Regulators of Actinobacteria: Phylogenomic Distribution and Functional Diversity. *PLoS One 7*, No. e46758.

(43) Venturi, V., and Ahmer, B. M. M. (2015) Editorial: LuxR Solos Are Becoming Major Players in Cell−Cell Communication in Bacteria. *Front. Cell. Infect. Microbiol. 5*, 89.

(44) Covaceuszach, S., Degrassi, G., Venturi, V., and Lamba, D. (2013) Structural Insights into a Novel Interkingdom Signaling Circuit by Cartography of the Ligand-Binding Sites of the Homologous Quorum Sensing LuxR-Family. *Int. J. Mol. Sci. 14*, 20578−20596.

(45) Higgins, S., Heeb, S., Rampioni, G., Fletcher, M. P., Williams, P., and Cámara, M. (2018) Differential Regulation of the Phenazine Biosynthetic Operons by Quorum Sensing in Pseudomonas Aeruginosa PAO1-N. *Front. Cell. Infect. Microbiol. 8*, 252.

(46) Frost, D. C., Greer, T., and Li, L. (2015) High-Resolution Enabled 12-Plex DiLeu Isobaric Tags for Quantitative Proteomics. *Anal. Chem. 87*, 1646−1654.

(47) Lu, W., Leimkuhler, C., Oberthür, M., Kahne, D., and Walsh, C. T. (2004) AknK Is an L-2-Deoxyfucosyltransferase in the Biosynthesis of the Anthracycline Aclacinomycin A. *Biochemistry 43*, 4548−4558.

(48) Garrido, L. M., Lombó, F., Baig, I., Nur-e-Alam, M., Furlan, R. L. A., Borda, C. C., Braña, A., Méndez, C., Salas, J. A., Rohr, J., and Padilla, G. (2006) Insights in the Glycosylation Steps during Biosynthesis of the Antitumor Anthracycline Cosmomycin: Charac-

DOI: 10.1021/acschembio.9b00223
ACS Chem. Biol. 2019, 14, 1260−1270

terization of Two Glycosyltransferase Genes. *Appl. Microbiol. Biotechnol. 73*, 122−131.
(49) Torkkell, S., Kunnari, T., Palmu, K., Hakala, J., Mäntsälä, P., and Ylihonko, K. (2000) Identification of a Cyclase Gene Dictating the C-9 Stereochemistry of Anthracyclines from Streptomyces Nogalater. *Antimicrob. Agents Chemother. 44*, 396−399.
(50) Torkkell, S., Kunnari, T., Palmu, K., Maè, P., Hakala, J., and Ylihonko, K. (2001) The Entire Nogalamycin Biosynthetic Gene Cluster of Streptomyces Nogalater : Characterization of a 20-Kb DNA Region and Generation of Hybrid Structures. *Mol. Genet. Genomics 266*, 276−288.
(51) Yoshimoto, A., Johdo, O., Takatsuki, Y., Ishikura, T., Sawa, T., Takeuchi, T., and Umezawa, H. (1984) New Anthracycline Antibiotics Obtained by Microbial Glycosidation of Beta-Isorhodomycinone and Alpha 2-Rhodomycinone. *J. Antibiot. 37*, 935−938.
(52) Wang, M., Carver, J. J., Phelan, V. V., Sanchez, L. M., Garg, N., Peng, Y., Nguyen, D. D., Watrous, J., Kapono, C. A., Luzzatto-Knaan, T., Porto, C., Bouslimani, A., Melnik, A. V., Meehan, M. J., Liu, W. T., Crüsemann, M., Boudreau, P. D., Esquenazi, E., Sandoval-Calderón, M., Kersten, R. D., Pace, L. A., Quinn, R. A., Duncan, K. R., Hsu, C. C., Floros, D. J., Gavilan, R. G., Kleigrewe, K., Northen, T., Dutton, R. J., Parrot, D., Carlson, E. E., Aigle, B., Michelsen, C. F., Jelsbak, L., Sohlenkamp, C., Pevzner, P., Edlund, A., McLean, J., Piel, J., Murphy, B. T., Gerwick, L., Liaw, C. C., Yang, Y. L., Humpf, H. U., Maansson, M., Keyzers, R. A., Sims, A. C., Johnson, A. R., Sidebottom, A. M., Sedio, B. E., Klitgaard, A., Larson, C. B., Boya P, C. A., Torres-Mendoza, D., Gonzalez, D. J., Silva, D. B., Marques, L. M., Demarque, D. P., Pociute, E., O'Neill, E. C., Briand, E., Helfrich, E. J. N., Granatosky, E. A., Glukhov, E., Ryffel, F., Houson, H., Mohimani, H., Kharbush, J. J., Zeng, Y., Vorholt, J. A., Kurita, K. L., Charusanti, P., McPhail, K. L., Nielsen, K. F., Vuong, L., Elfeki, M., Traxler, M. F., Engene, N., Koyama, N., Vining, O. B., Baric, R., Silva, R. R., Mascuch, S. J., Tomasi, S., Jenkins, S., Macherla, V., Hoffman, T., Agarwal, V., Williams, P. G., Dai, J., Neupane, R., Gurr, J., Rodríguez, A. M. C., Lamsa, A., Zhang, C., Dorrestein, K., Duggan, B. M., Almaliti, J., Allard, P. M., Phapale, P., Nothias, L. F., Alexandrov, T., Litaudon, M., Wolfender, J. L., Kyle, J. E., Metz, T. O., Peryea, T., Nguyen, D. T., VanLeer, D., Shinn, P., Jadhav, A., Müller, R., Waters, K. M., Shi, W., Liu, X., Zhang, L., Knight, R., Jensen, P. R., Palsson, B. O., Pogliano, K., Linington, R. G., Gutiérrez, M., Lopes, N. P., Gerwick, W. H., Moore, B. S., Dorrestein, P. C., and Bandeira, N. (2016) Sharing and Community Curation of Mass Spectrometry Data with Global Natural Products Social Molecular Networking. *Nat. Biotechnol. 34*, 828−837.
(53) Shannon, P., Markiel, A., Ozier, O., Baliga, N. S., Wang, J. T., Ramage, D., Amin, N., Schwikowski, B., and Ideker, T. (2003) Cytoscape: A Software Environment for Integrated Models of Biomolecular Interaction Networks. *Genome Res. 13*, 2498−2504.
(54) Medema, M. H., and Fischbach, M. A. (2015) Computational Approaches to Natural Product Discovery. *Nat. Chem. Biol. 11*, 639−648.
(55) Chung, J.-Y., Fujii, I., Harada, S., Sankawa, U., and Ebizuka, Y. (2002) Expression, Purification, and Characterization of AknX Anthrone Oxygenase, Which Is Involved in Aklavinone Biosynthesis in Streptomyces Galilaeus. *J. Bacteriol. 184*, 6115−6122.
(56) Tang, G.-L., Cheng, Y.-Q., and Shen, B. (2004) Leinamycin Biosynthesis Revealing Unprecedented Architectural Complexity for a Hybrid Polyketide Synthase and Nonribosomal Peptide Synthetase. *Chem. Biol. 11*, 33−45.
(57) Zhang, W., Wang, L., Kong, L., Wang, T., Chu, Y., Deng, Z., and You, D. (2012) Unveiling the Post-PKS Redox Tailoring Steps in Biosynthesis of the Type II Polyketide Antitumor Antibiotic Xantholipin. *Chem. Biol. 19*, 422−432.
(58) Galm, U., Wang, L., Wendt-Pienkowski, E., Yang, R., Liu, W., Tao, M., Coughlin, J. M., and Shen, B. (2008) Vivo Manipulation of the Bleomycin Biosynthetic Gene Cluster in Streptomyces Verticillus ATCC15003 Revealing New Insights into Its Biosynthetic Pathway. *J. Biol. Chem. 283*, 28236−28245.
(59) Ogasawara, Y., and Liu, H. (2009) Biosynthetic Studies of Aziridine Formation in Azicemicins. *J. Am. Chem. Soc. 131*, 18066−18068.
(60) Ge, H.-M., Huang, T., Rudolf, J. D., Lohman, J. R., Huang, S.-X., Guo, X., and Shen, B. (2014) Enediyne Polyketide Synthases Stereoselectively Reduce the *β*-Ketoacyl Intermediates to *β*-d-Hydroxyacyl Intermediates in Enediyne Core Biosynthesis. *Org. Lett. 16*, 3958−3961.
(61) August, P. R., Tang, L., Yoon, Y. J., Ning, S., Müller, R., Yu, T.-W., Taylor, M., Hoffmann, D., Kim, C.-G., Zhang, X., Hutchinson, C. R., and Floss, H. G. (1998) Biosynthesis of the Ansamycin Antibiotic Rifamycin: Deductions from the Molecular Analysis of the Rif Biosynthetic Gene Cluster of Amycolatopsis Mediterranei S699. *Chem. Biol. 5*, 69−79.
(62) Alvarez-Mico, X., Jensen, P. R., Fenical, W., and Hughes, C. C. (2013) Chlorizidine, a Cytotoxic 5 *H* -Pyrrolo[2,1- *a*]Isoindol-5-One-Containing Alkaloid from a Marine *Streptomyces* Sp. *Org. Lett. 15*, 988−991.
(63) Mantovani, S. M., and Moore, B. S. (2013) Flavin-Linked Oxidase Catalyzes Pyrrolizine Formation of Dichloropyrrole-Containing Polyketide Extender Unit in Chlorizidine A. *J. Am. Chem. Soc. 135*, 18032−18035.
(64) Kang, Q., Shen, Y., and Bai, L. (2012) Biosynthesis of 3,5-AHBA-Derived Natural Products. *Nat. Prod. Rep. 29*, 243−263.
(65) He, W., Lei, J., Liu, Y., and Wang, Y. (2008) The LuxR Family Members GdmRI and GdmRII Are Positive Regulators of Geldanamycin Biosynthesis in Streptomyces Hygroscopicus 17997. *Arch. Microbiol. 189*, 501−510.
(66) Braesel, J., Crnkovic, C. M., Kunstman, K. J., Green, S. J., Maienschein-Cline, M., Orjala, J., Murphy, B. T., and Eustáquio, A. S. (2018) Complete Genome of Micromonospora Sp. Strain B006 Reveals Biosynthetic Potential of a Lake Michigan Actinomycete. *J. Nat. Prod. 81*, 2057−2068.
(67) Langmead, B., and Salzberg, S. L. (2012) Fast Gapped-Read Alignment with Bowtie 2. *Nat. Methods 9*, 357−359.
(68) Seemann, T. (2014) Prokka: Rapid Prokaryotic Genome Annotation. *Bioinformatics 30*, 2068−2069.
(69) Huson, D. H., and Weber, N. (2013) Microbial Community Analysis Using MEGAN. *Methods Enzymol. 531*, 465−485.
(70) Miller, I. J., Vanee, N., Fong, S. S., Lim-Fong, G. E., and Kwan, J. C. (2016) Lack of Overt Genome Reduction in the Bryostatin-Producing Bryozoan Symbiont "Candidatus Endobugula Sertula". *Appl. Environ. Microbiol. 82*, 6573−6583.
(71) Adnani, N., Vazquez-Rivera, E., Adibhatla, S., Ellis, G., Braun, D., and Bugni, T. (2015) Investigation of Interspecies Interactions within Marine Micromonosporaceae Using an Improved Co-Culture Approach. *Mar. Drugs 13*, 6082−6098.
(72) Styles, M. J., and Blackwell, H. E. (2018) Non-Native Autoinducer Analogs Capable of Modulating the SdiA Quorum Sensing Receptor in *Salmonella Enterica* Serovar Typhimurium. *Beilstein J. Org. Chem. 14*, 2651−2664.
(73) Eibergen, N. R., Moore, J. D., Mattmann, M. E., and Blackwell, H. E. (2015) Potent and Selective Modulation of the RhlR Quorum Sensing Receptor by Using Non-Native Ligands: An Emerging Target for Virulence Control in *Pseudomonas Aeruginosa*. *ChemBioChem 16*, 2348−2356.

DOI: 10.1021/acschembio.9b00223
ACS Chem. Biol. 2019, 14, 1260−1270